

Article

Evaluation of Agricultural Soil-Improving Zeolite for Improving Irrigation Water Quality

Dámaris Núñez-Gómez , Pilar Legua , Vicente Lidón, Agustín Conesa , Juan José Martínez-Nicolás * 
and Pablo Melgarejo 

Plant Production and Microbiology Department, Miguel Hernandez University (UMH), Ctra. Beniel km 3.2, 03312 Orihuela, Alicante, Spain; dnunez@umh.es (D.N.-G.); p.legua@umh.es (P.L.); vicente.lidon@umh.es (V.L.); agustin.conesa@umh.es (A.C.); pablo.melgarejo@umh.es (P.M.)

* Correspondence: juanjose.martinez@umh.es

Abstract: With a progressively decreasing availability of water for irrigation, the utilization of lower agronomic quality water sources is becoming more prevalent. Compounds such as sodium and boron, due to their impact on crop development and production, are gaining significance in these water sources. Finding novel methods to immobilize these compounds in irrigation water is a top priority in the global agricultural sector. This study focused on exploring the potential of natural zeolite, commonly used as a soil improver and as a sorbent for sodium and boron in natural agricultural waters. The zeolite exhibited favorable properties, including a surface area of 40 m²/g and a cation-exchange capacity of 1.8 mg/g. Using a central composite factorial design, the zeolite's capacity to remove sodium and boron from irrigation water was investigated. The results demonstrated significant efficiency in boron removal, while sodium removal was limited, with occasional desorption episodes. Response surface analysis revealed optimal conditions for the removal of each cation. Additionally, adsorption kinetics and pH effects were explored, emphasizing the influence on sodium sorption. Kinetic models were applied, and the pseudo-first-order model proved suitable for describing the sorption kinetics. These findings enhance our understanding of zeolite efficacy in irrigation water purification, emphasizing the complexity of cation interactions in “complex” solutions.

Keywords: sorption; sorption kinetics; irrigation water; central composite factorial design; cation removal



Citation: Núñez-Gómez, D.; Legua, P.; Lidón, V.; Conesa, A.; Martínez-Nicolás, J.J.; Melgarejo, P. Evaluation of Agricultural Soil-Improving Zeolite for Improving Irrigation Water Quality. *Appl. Sci.* **2024**, *14*, 418. <https://doi.org/10.3390/app14010418>

Academic Editor: Jan Yperman

Received: 28 November 2023

Revised: 27 December 2023

Accepted: 31 December 2023

Published: 3 January 2024



Copyright: © 2024 by the authors. Licensee MDPI, Basel, Switzerland. This article is an open access article distributed under the terms and conditions of the Creative Commons Attribution (CC BY) license (<https://creativecommons.org/licenses/by/4.0/>).

1. Introduction

The discovery of natural zeolites has opened a significant chapter in the field of mineralogy, owing to their intriguing surface and structural properties that have been exploited in various sectors, including agriculture, industrial technology, livestock, cosmetics, and the biotechnological industry [1].

Zeolites form a large family of minerals and are among the most important in terms of microporous materials. The term “zeolite” refers to a polymorph of crystalline silica or aluminosilicate based on various tetrahedral TO₄ units that share corners (T = typically silicon and aluminum), forming a three-dimensional structure with regularly sized molecular dimension pores [1,2]. More than 50 different species have been identified within this mineral group, with more yet to be discovered. Zeolites have been classified based on their morphological features, crystalline structure, chemical composition, effective pore diameter, natural occurrence, and other criteria [3,4]. The Si/Al ratio is an important characteristic of zeolites. The charge imbalance resulting from the presence of aluminum in the zeolite structure determines the ionic exchange characteristics of zeolites and is expected to induce potential acidic sites. The Si/Al ratio is inversely proportional to the cation content but directly proportional to thermal stability [3]. Among natural zeolites, clinoptilolite [5] stands out, commonly used in agricultural practices as a soil amendment and to promote nitrogen retention in soils [1,6,7].

On the other hand, water is one of the essential substances for development, especially in arid and semi-arid regions of the world where renewable water resources are scarce [2]. Among the various sectors that consume freshwater, agricultural farms are considered the primary consumers, using more than two-thirds of renewable water resources in these activities [8]. Additionally, population growth demands greater food quantities, making efficient cultivation crucial to sustain urban development. While high-efficiency agricultural activities are needed to meet current food demands, several issues have emerged in achieving this goal, primarily related to irrigation and, importantly, the quality of agricultural waters.

The quality of water used for crop irrigation is a crucial factor that can have a significant impact on agricultural productivity and soil health [9,10]. It is due to its importance that the FAO has been conducting the review and updating of its “Water Quality for Agriculture” report since 1976 [11]. This document serves as a field guide for assessing the suitability of water for irrigation and addresses issues such as the following:

- **Water Salinity:** Salinity is a critical factor. If the water used for irrigation has a high salt content, it can accumulate in the soil as water evaporates, affecting the plant’s ability to absorb water and nutrients. This can lead to soil salinization and reduce crop yields.
- **Infiltration and Drainage:** Water quality also affects the rate of water infiltration into the soil and drainage. If the water is of low quality and contains sodium, it can affect soil structure, decrease infiltration, and cause drainage problems. This can result in compacted soil and waterlogging, negatively affecting plant growth.
- **Toxicity of Specific Ions:** Some ions present in water, such as sodium, chloride, and boron, can become toxic to plants at high concentrations. This can affect plant development and reduce yields.
- **Effects on Soil Health:** Poor water quality can contribute to long-term soil degradation. The accumulation of salts, loss of soil structure, and reduced biological activity can impact overall soil health.
- **Sustainability of Irrigation:** Sustainable water management is essential for long-term agriculture. The use of poor-quality water without proper management can deplete water resources and have negative environmental consequences.
- **Impact on Crop Quality:** Water quality can also influence the quality of agricultural products. High concentrations of salts or toxic ions can affect the taste and appearance of crops, which are critical in fresh produce markets.

Among the elements posing significant challenges for removal or reduction in agricultural waters, two stand out: sodium and boron. Sodium can harm crops by creating short-term osmotic stress or causing long-term direct toxicity. As the osmotic pressure decreases in saline soils, plant turgor pressure is affected and tissues dehydrate, slowing down photosynthesis and leading to inhibited growth, biomass loss, a significant reduction in production, and, ultimately, death [12]. On the other hand, although boron is a necessary micronutrient for the growth and development of plants in very small amounts, exceeding these levels, either through continuous input in irrigation, soil, etc., or through bioaccumulation in the plant organism, can result in various toxic effects, depending on the crops, such as leaf chlorosis and necrosis, root weakness, and death [13–15].

In this context, the present study aimed to investigate the sorption of boron and sodium found in natural agricultural waters on commercial clinoptilolite-type zeolite, commonly used as a soil conditioner. The goal was to identify the zeolite’s retention potential for these two phytotoxic cations in crops, providing a complementary and/or secondary benefit to soil improvement, such as water retention, increased oxygen, and nitrogen mobilization. The study of the process and the identification of the optimal experimental conditions were conducted through factorial planning. Additionally, a kinetic study was carried out to investigate the optimal contact time for the sorbent/cation and the sorption mechanisms that best describe the process.

It is emphasized that, despite the abundance of available studies focused on the sorption capacity of zeolite [16–19], to date, no research has been found that works with real irrigation waters, which are considered complex due to the diversity of chemical and

biological elements they contain. Furthermore, none of these studies concurrently focused on the two chemical species that are most “problematic” in agriculture, sodium and boron, given their negative impact on plant growth and, consequently, on production.

2. Materials and Methods

2.1. Adsorbent Characterization

For this study, commercially available natural zeolite of the clinoptilolite type, specifically FERTCEL zeolite (Zeocel Ltda., Águeda, Portugal), was employed. Widely utilized in agriculture to regulate soil fertility, maximize nutrient utilization, and qualitatively and quantitatively improve crop yields, this zeolite boasts a high cation-exchange capacity (CTC) exceeding 150 mEq/100 g, temporarily retaining ions and releasing them as required by plants. According to the manufacturer’s data, it reduces nitrogen losses in the soil, prevents phosphorus fixation by iron, aluminum, and manganese in acidic soils, enhances potassium efficiency, and mitigates soil acidity. Additionally, it can absorb up to 40% of its weight in water. The physicochemical and mineralogical characterization of clinoptilolite zeolite (hydrated aluminosilicate) was conducted in an independent laboratory specializing in chemical–agricultural analyses, accredited by the National Accreditation Entity (ENAC, Madrid, Spain), ensuring the objectivity of the results.

In this context, the crystalline phases of the zeolite were assessed through X-ray diffraction (XRD, Bruker-AXR D8 Advance) under the following conditions: $\Delta 2\theta = 5\text{--}65^\circ$, 2° increments, integration time = 0.05 s, Cu K α 1 radiation, $\lambda = 1.540598 \text{ \AA}$ [20]. The obtained diffractograms were analyzed and compared with the Crystallography Open Database (COD, available at <http://www.crystallography.net/> (accessed on 27 December 2023) using the specialized software Match! version 3.16. The chemical composition was determined through Fourier-transform infrared spectroscopy (FTIR-4700 type A, FTIR spectrometer JASCO Quick Start System with ATR Pro One as an accessory). Spectra were collected with a resolution of 4 cm^{-1} in the range of 400 cm^{-1} to 1400 cm^{-1} and analyzed using OriginPro 9.5 Software (OriginLab Corporation, Northampton, USA) [21,22]. Furthermore, laser diffraction techniques (Master Sizer 2000, APA2000 model from Malvern Instruments Ltd., Cambridge, UK) in the range of 0.01 to 3500 \mu m were employed [23].

2.2. Irrigation Water Characterization

In pursuit of elucidating the retention and/or immobilization capacity of boron and sodium—elements commonly prevalent in irrigation waters and notorious for their adverse effects on agriculture, particularly in citrus cultivation—samples were drawn from an irrigation reservoir situated on a commercial citric farm in Ojós municipality, Murcia, Spain. The preference for these authentic natural waters rested on their compositional intricacies, posing a significant challenge to replicate accurately in laboratory conditions using synthetic counterparts. The presence or absence of diverse compounds and contaminants in these waters can distinctly shape, modify, or entirely transform the reactions and interactions of dissolved species [24].

The irrigation water samples, obtained in non-sterile 15 L polypropylene containers from accessible points in the reservoir, were immediately transported and stored at a constant temperature of $4 \text{ }^\circ\text{C}$ until their characterization and use on the same collection day. A rigorous characterization of all irrigation water samples was carried out before and after the experiments using inductively coupled plasma mass spectrometry (ICP-MS Model 2030, Shimadzu, Kyoto, Japan), selected for its precision and well-established recognition in the characterization of liquid samples. Additionally, continuous real-time monitoring and characterization of all agronomically significant ions (sodium, potassium, pH, electrical conductivity, chloride, nitrate, magnesium, calcium, and ammonium, among others) present in the effluents were meticulously carried out throughout the experiments. This detailed monitoring was conducted using the Imacimus Multi Ion 10 portable multi-ion nutrient analyzer (Imacimus NT Sensors, El Catllar, Spain), which provides readings of the agronomic parameters of interest every 2 min. It is noteworthy that this probe is

specialized for field measurements and is widely utilized in the agricultural estates of the region [25,26].

2.3. Statistical Factorial Design

Aiming to determine the optimal system configuration while minimizing the total number of experiments required, a preliminary factorial design was conducted. This design identified factors with significant effects on response and elucidated how a factor's impact varies, considering the levels of other factors. The exploration of interactions between factors necessitates the application of statistical experimental designs, as optimizing the system cannot be achieved by varying one factor at a time while keeping other factors constant [27,28]. In this sense, and aiming to optimize the process, a central composite rotatable design (CCRD) with two factorial variables (2^2) was employed, where the zeolite content (g/L) and contact time (min) served as independent variables, while sodium (Na) and boron (B) concentrations constituted the dependent or response variables. A total of 12 batch experiments were conducted by the statistical design matrix and the studied factorial levels, as presented in Table 1. To minimize experimental error, the study included a quadruplicate repetition of the central point. Initial levels for the factorial setup were determined based on the literature [29–33]. Once the effective range of removal variables was identified through a bibliographic review, preliminary removal assays were conducted by the same scientific team (unpublished data). Building upon the outcomes of these preliminary assays, the minimum and maximum adsorbent content for use in this study were subsequently established. The values for the axial points (-1.4142 and $+1.4142$) were determined through interpolation by the model's methodology [27,34].

Table 1. Factorial design (2^2) results for sodium and boron retention in waters intended for agricultural irrigation, where X_1 and X_2 represent the variable levels for zeolite content and contact time, respectively.

Run	X_1	X_2	Zeolite Content (g/L)	Contact Time (min)
1	−1	−1	12.43	194.33
2	1	−1	54.84	194.33
3	−1	1	12.43	765.67
4	1	1	54.84	765.67
5	0	0	33.64	480.00
6	0	0	33.64	480.00
7	0	0	33.64	480.00
8	0	0	33.64	480.00
9	−1.4142	0	3.64	480.00
10	0	−1.4142	33.64	76.00
11	1.4142	0	63.63	480.00
12	0	1.4142	33.64	884.00

All experiments were conducted at a constant temperature of 22 ± 2 °C. Each trial involved using 100 mL of liquid sample in non-sterile polypropylene Erlenmeyer flasks with a maximum capacity of 250 mL and a standardized neck (Kartell Labware, Noviglio, Italy). Cellulose acetate membranes of 0.20 μm and 47 mm in diameter (Teknokroma, Barcelona, Spain) were employed for sample water filtration.

The experimental data were analyzed using appropriate statistical methods for the applied experimental design. Mathematical models for each response were assessed through multiple linear regression analysis and were processed using STATISTICA 18 software from StatSoft (TIBCO Software Inc., Palo Alto, CA, USA). Statistically significant terms in the model, whether linear or nonlinear, were determined through analysis of variance (ANOVA) for each response, with a significance level set at $p < 0.05$ (95% confidence).

Identifying the significant factors in the model allowed for a reliable prediction of performance through interpolation across a range of data, facilitating the construction of response surface graphs (3D). These graphs contribute to a better understanding of the investigated process [35].

2.4. Batch Kinetic Sorption Tests

Based on the results obtained from the experimental factorial design, kinetic sorption tests were conducted to identify and define the most appropriate kinetics that describe the process. This knowledge is crucial, as it provides valuable information about the mechanism of the process and indicates the sorption rate, which, in treating an effluent, determines the residence time of the sorbate at the interface between the solution and the sorbent material.

For this purpose, 100 mL of irrigation water was placed in non-sterile polypropylene Erlenmeyer flasks with a maximum capacity of 250 mL, containing 4.93 g of zeolite/L, and a total contact time of 6200 min at a constant controlled temperature (22 ± 1 °C). In all cases, the flasks were covered with a transparent biofilm to prevent dust and/or impurities from entering. The quantity of zeolite and the total contact time were predetermined through factorial experimental planning.

At various predefined times, each Erlenmeyer flask was opened for sampling and monitoring of cation concentrations. A total of 17 tests were conducted. Before the characterization analyses, the aqueous samples were filtered with cellulose acetate filters of 0.20 µm and 47 mm in diameter (Teknokroma, Barcelona, Spain). The percentage removal of sodium and boron was determined using Equation (1), where C_0 and C_t represent the initial concentration of cations and the concentration at time t (mg/L), respectively.

$$\% \text{ removal} = \frac{C_0 - C_t}{C_0} \times 100 \quad (1)$$

The assessment of the kinetic mechanism of the sorption process was conducted by applying the three most commonly used kinetic models to the experimental data. These models are (i) Lagergren's pseudo-first-order model, commonly employed for liquid-solid sorption, as it considers the rate of occupation of active sites to be proportional to the number of available active sites in the adsorbent material, also known as physisorption [36,37]; (ii) Ho and McKay's pseudo-second-order model, based on solid-phase sorption, presupposing it as a chemical sorption process involving the participation of valence forces or electron exchange between sorbate and sorbent, thus describing chemisorption [38]; and (iii) Weber and Morris's intraparticle diffusion model, wherein the limiting stage of the sorption process may be caused by the slowness of the intraparticle diffusion mechanism [39]. The corresponding equations of the kinetic models are shown in Table 2.

Table 2. Equations of kinetic models used in this study.

Model	Equation
Pseudo-first-order	$\frac{dq_t}{dt} = k_1(q_e - q_t)$
where q_e and q_t represent the amounts of sorbate retained (mg) per gram of sorbent at equilibrium and time t , respectively, and k_1 (min^{-1}) is the rate constant of the pseudo-first-order.	
Pseudo-second-order	$\frac{dP_t}{dt} = k(HP_e - HP_t)^2$
where P_t and HP_t correspond to the number of occupied active sites on the sorbent at time t , while P_e y HP_e refers to the number of available active sites on the sorbent at equilibrium.	
Intraparticle diffusion	$q_t = k_{in}t^{\frac{1}{2}} + C$
where k_{in} is the rate of intraparticle diffusion ($\text{mg g}^{-1} \text{min}^{-0.5}$) and C is the constant related to the thickness of the diffusion layer (mg g^{-1}).	

3. Results and Discussion

3.1. Zeolite Characterization

The compositional and mineralogical characterization of the zeolite used indicated a composition of 98% clinoptilolite and 2% modernite, with a chemical composition mainly consisting of silica, alumina, and lime (Table 3).

Table 3. Average chemical composition (%) and physical characteristics of the natural zeolite used. Mean values with standard deviation in parentheses.

Chemical Composition (%)										
SiO ₂	Al ₂ O ₃	CaO	Na ₂ O	Fe ₂ O ₃	FeO	K ₂ O	TiO ₂	MgO	P ₂ O ₅	pH
63.00 (3.00)	11.57 (1.20)	5.78 (0.62)	2.39 (0.26)	1.82 (0.81)	0.81 (0.02)	1.49 (0.40)	0.45 (0.01)	0.92 (0.53)	0.09 (0.01)	8.2
Physical Characteristics										
Surface area						m ² /g	40			
Bulk density						g/L	0.98			
Cation-exchange capacity						mg/g	1.8			
Particle size						mm	1.0–2.5			

The pH was slightly higher than the manufacturer's indication (7.6), possibly due to the natural variation in its composition. In general, an adsorbent is considered effective when it exhibits a large surface area, excellent physical, chemical, and mechanical stability, and selectivity/ease of binding to certain compounds of interest [40]. In this regard, the zeolite samples showed a surface area of 40 m²/g. This value was higher than that of other natural zeolites (10 m²/g) [41] and synthetic zeolites intended for the removal of Pb (II) and Cu (II) (19.17 m²/g). However, it was significantly lower than that of synthetic zeolitic nanocomposites (ranging from 103 to 434 m²/g) designed primarily for the removal of dyes and emerging contaminants [42–45].

It is widely known that zeolite possesses an excellent cation-exchange capacity (CEC), and the cations within the zeolite significantly influence its characteristics and, therefore, its application [46,47]. The CEC values in the samples used are in line with those reported for natural zeolites [41,48].

3.2. Irrigation Water Characterization

The comprehension of water quality empowers farmers and project managers to make judicious decisions concerning the volume and frequency of irrigation. Furthermore, it enables the implementation of apt management practices aimed at mitigating adverse impacts.

The average pH of the irrigation water before treatment was approximately 8.35. The chemical characterization of the initial samples is shown in Table 4, where the obtained values are compared with the maximum limits for irrigation water defined by the FAO [11], as well as the restrictions on water use for irrigation [11,49]. Among all identified elements, only sodium and boron presented higher usage restrictions due to their high concentrations. Thus, in this case, only boron and sodium were evaluated, as the other elements were within permissible limits for agricultural water use.

It is crucial to emphasize that, in the present study, water characteristics and the criteria for suitability and adequacy for use as irrigation water are based on the FAO document "Water Quality for Agriculture" That report not only presents water-quality guidelines for irrigation, supported by specialized scientific-technical reports, but also establishes, defines, and indicates potential restrictions for its use. The approach in the document underscores a problem-solving perspective and highlights the importance of comprehending the long-term effects of low-quality water in agriculture. The text also

provides laboratory tools for assessing water quality and underscores that the guidelines are management tools, requiring adaptability based on local conditions.

Table 4. Chemical characterization of irrigation water before treatment. Values compared with FAO irrigation water-quality standards [11]. The results represent the mean values ($n = 5$), with standard deviations in parentheses.

	Water Samples	Limit Irrigation Water (FAO)	Restriction Use (FAO)
pH		6–8.5	-
CE (dS/m)	1.3 (0.2)	0–3	Medium
Ca ²⁺ (meq/L)	15.1 (2.8)	0–20	-
Na ⁺ (meq/L)	9.7 (0.2)	0–40	High
Mg ²⁺ (meq/L)	1.1 (0.4)	0–5	-
CO ₃ ²⁻ (meq/L)	<0.1	0–0.1	-
Cl (meq/L)	5.24 (1.4)	0–30	Medium
NO ₃ (mg/L)	6.6 (1.2)	0–10	Medium
NH ₄ ⁺ (mg/L)	5.4 (0.9)	0–2	-
K ⁺ (mg/L)	10.2 (1.0)	0–2	-
B (mg/L)	0.75 (0.3)	0–2	High
SAR (meq/L)	9.2	0–15	Medium

In most cultivated plant species [13], toxicity symptoms typically manifest as chlorotic. As mentioned earlier, boron is an essential micronutrient for plant development [14,50]. However, the threshold between the concentration required for proper plant development (0.3–0.5 ppm) is very close to the levels that exhibit toxicity, ranging from 0.6 ppm to 1.0 ppm manifestations in leaves, phenotypically similar to leaf burns, with an initial appearance at the margins and subsequent expansion toward the basal portion [13,51].

On the other hand, sodium, which is the main element in water and/or soil salinity, has significant negative impacts on plant development, primarily due to the increase in soil osmotic pressure, which directly interferes with plant nutrition by reducing the plant's ability to adsorb water, altering the homeostasis of root cell ions [52,53]. Munns et al. [54] categorized the damage caused by excessive salt presence as identical to that caused by water stress-induced "wilting". Moreover, various studies indicated a direct relationship between salinity and photosynthesis, as it limits CO₂ diffusion and reduces photosynthetic pigment content [55,56]. More specifically, in the case of citrus, as early as 1993, Maas [57] highlighted how soil salinity significantly limits citrus production. The author indicated a reduction of about 13% in production for every 1.0 dS/m increase in the electrical conductivity of the saturated soil extract from 1.4 dS/m.

The assessment of sodium concentration as the sodium adsorption ratio (SAR) is important when considering water suitability for irrigation, as it affects soil salinity, hardness, and infiltration rate [58,59]. The higher the concentrations of Na relative to Ca and Mg, the higher the SAR will be.

3.3. Central Composite Rotatable Design (CCRD)

The results revealed distinct behaviors for each of the studied species. While several tested conditions achieved 100% removal of boron (B), sodium (Na) removal percentages were considerably lower, ranging from 10% to 24%. In one of the trials, desorption or release of sodium was observed, leading to a final sodium concentration 147% higher than the initial concentration (Table 5). This underscores the suitability of the factorial design for boron removal via zeolite but emphasizes its limited efficacy for combined sodium removal. The results suggest the interaction and influence of the presence of other chemical species,

both in the irrigation water samples and in the zeolite composition itself [24]. Shuangtan et al. [60] previously reported cyclic episodes of sodium adsorption/desorption in zeolite compounds, primarily due to the large ionic diameter of the sodium cation (1.02 Å), causing a significant expansion of the material volume to accommodate sodium. However, the same study indicated the potential for sodiation and desodiation of zeolitic materials during multiple cycles.

Table 5. Factorial design (2^2) results for sodium and boron removal (%) in irrigation water through zeolite treatment.

Run	X_1	X_2	Zeolite Content (g/L)	Contact Time (min)	Na Removal (%)	B Removal (%)
1	−1	−1	12.43	194.33	16%	67%
2	1	−1	54.84	194.33	6%	67%
3	−1	1	12.43	765.67	−147%	89%
4	1	1	54.84	765.67	17%	67%
5	0	0	33.64	480.00	10%	100%
6	0	0	33.64	480.00	22%	100%
7	0	0	33.64	480.00	15%	100%
8	0	0	33.64	480.00	11%	100%
9	−1.4142	0	3.64	480.00	15%	94%
10	0	−1.4142	33.64	76.00	24%	67%
11	1.4142	0	63.63	480.00	16%	98%
12	0	1.4142	33.64	884.00	14%	95%

The divergent behavior of species with zeolite was once again confirmed in the estimation of significant effects at a 95% confidence interval. As observed in Table 6, for sodium, none of the studied dependent variables or their interaction proved to be significant. In contrast, for boron removal via zeolite, both linear and quadratic forms of contact time were statistically significant.

Table 6. Estimated effects for variables in sodium (Na) and boron (B) removal via zeolite.

	Coefficient	Effect	Standard Error	t (2)	p-Value
[Na]					
Zeolite content (L)	Q_1	0.39	0.28	1.39	0.21
Zeolite content (Q)	Q_1^2	−0.21	0.31	−0.67	0.52
Contact time (L)	Q_2	−0.42	0.28	−1.49	0.18
Contact time (Q)	Q_2^2	−0.18	0.31	−0.56	0.59
Zeolite content vs. contact time	Q_1 vs. Q_2	0.87	0.40	2.21	0.06
[B]					
Zeolite content (L)	Q_1	−0.08	0.07	−1.1	0.32
Zeolite content (Q)	Q_{12}	−0.08	0.08	−0.96	0.37
Contact time (L)	Q_2	0.19	0.07	2.6	0.04
Contact time (Q)	Q_{22}	−0.24	0.08	−2.89	0.02
Zeolite content vs. contact time	Q_1 vs. Q_2	−0.16	0.1	−1.52	0.17

where (L) and (Q) represent the linear and quadratic forms, respectively.

For both species, negative and positive response relationships with the variables were observed. Specifically, zeolite content and contact time, both in their quadratic forms (Q_{12} and Q_{22}), exhibited a negative relationship with the variable. In linear forms, contact time (Q_2) for sodium and zeolite content (Q_1) for boron also displayed a negative relationship. The interaction of other responses with the variables was positive (Table 6). Positive-effect values mean that an increase in their levels leads to an increase in ionic sorption, while negative values result in a decrease in the response as their levels increase [61].

Based on the significant variables, an analysis of variance (ANOVA) for the entire statistical model was conducted (Table 7). It was necessary to adjust confidence values when evaluating both independent variables simultaneously to confirm that $F_{Cal} > F_{Tab}$. In this regard, the ANOVA results indicated that for sodium removal, the confidence interval was 75%, while for boron, it remained at 90% (Table 7).

Table 7. Analysis of variance for sodium and boron removal variables resulting from the 2^2 factorial design.

Variation Source	SS	d.f	MS	F Cal	F Tab ^a	<i>p</i>
Na removal						
Regression	1.53	5	1.53	1.97	1.79	<0.25
Sediments	0.93	6	0.15			
Total	2.43	11				
B removal						
Regression	0.227	5	0.227	3.89	3.11	<0.1
Sediments	0.07	6	0.012			
Total	0.29	11				

SS—sum of squares; d.f.—degrees of freedom; MS—mean square; F—Fisher's ratio; *p*—probability. ^a Values are tabulated according to Box et al. [62].

Based on the linear coefficients, quadratic coefficients, and their interactions, it is possible to conduct the response surface analysis, which helps identify the most appropriate conditions to maximize the removal of the studied cations using the desirability function for multiple response optimization [35,61,63].

The 3D response surface plots are shown in Figure 1, once again highlighting the differentiated response of each cation. The maximum sodium removal values were established at around 50% with a zeolite content of up to 10 g/L or between 60–70 g/L, and a contact time of up to 100 min or between 800–1000 min, respectively. However, with a zeolite content of up to 35 g/L and a contact time exceeding 500 min, potential desorption and/or release of sodium by the zeolite was observed, resulting in negative removal values. This situation was observed again with a shorter contact time, up to 200 min, but a higher zeolite content (<55 g/L). Removal of boron, on the other hand, showed a higher response when longer contact times were applied (between 600 and 800 min), displaying a central zone of high removal (> 95%), with a zeolite content of up to 50 g per liter. However, according to Figure 1B, contents ≤ 20 g of zeolite/L allowed for maximum boron removal (100% removal). In all scenarios, with low contact times (≤ 300 min), the removal efficiency was significantly impacted.

Based on the obtained results, the statistically defined critical values for the maximum efficiency of the cation removal process from irrigation water using zeolite were determined. Due to their differentiated behavior, the critical values were chosen based on the experimental design for boron, confirmed by ANOVA of the model at a 90% confidence interval and presenting the highest sorption percentages with zeolite. Thus, 4.93 g of zeolite/L and 723 min were determined as the best theoretical conditions for the studied process. Regardless of the statistical definition of experimental conditions, the removal/immobilization of sodium in zeolite was also studied and evaluated in the subsequent stages to identify the

overall behavior of the “complex” water and its potential impact on the concentration in irrigation water as an additional positive aspect.

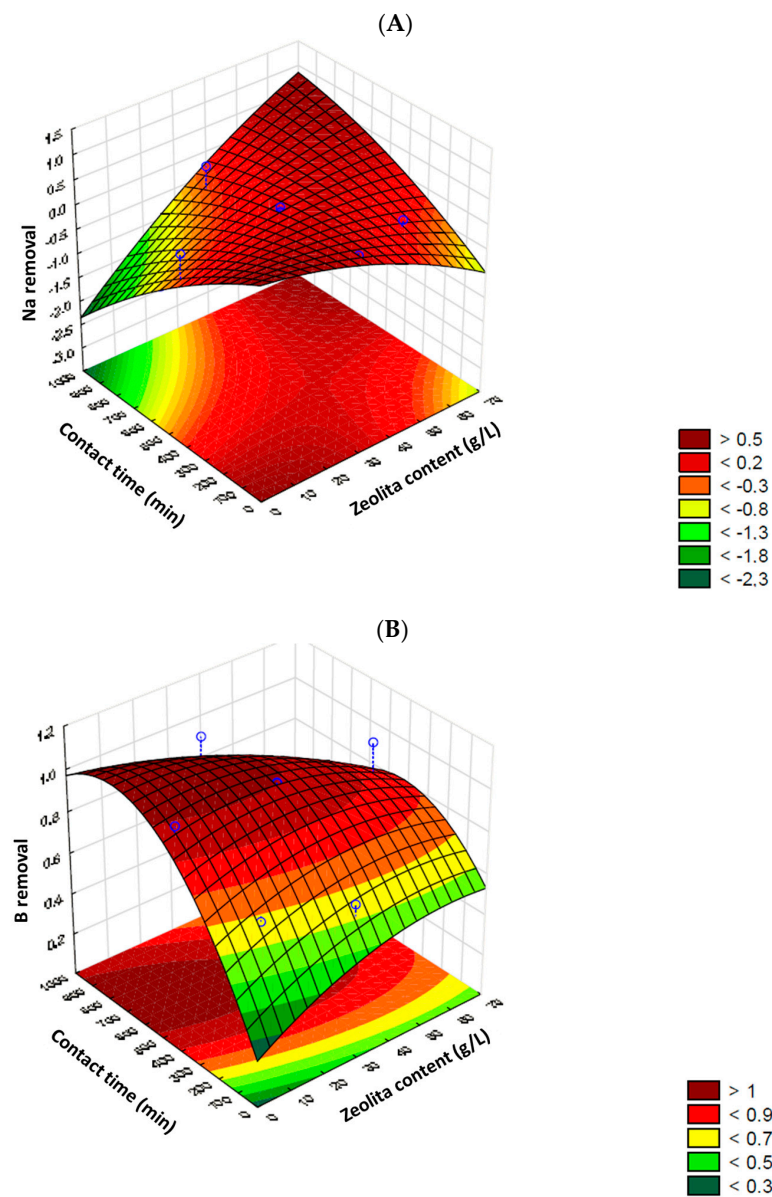


Figure 1. 3D Response surface plots for sodium (A) and boron (B) removal, considered individually.

3.4. Adsorption Kinetics

The kinetics are influenced by the sorption mechanism and the mass transfer steps governing the transfer of cations from the solution to the sorption sites on the surface and within the adsorbent particles, i.e., external and intraparticle diffusion. In turn, these mechanisms depend on the physical form of the sorbent (mainly particle size and pores)—in this case, zeolite, its intrinsic structure, the nature of the cation and the solution, and the process conditions (contact time and zeolite content). Simplified models can be used to test batch experimental data and identify the rate-controlling mechanisms for the adsorption process [61]. In this study, the three most common kinetic models were applied and studied.

3.4.1. Contact Time

The relationship between contact time and the sorption of B and Na was analyzed according to the conditions identified by the CCRD. The results (Figure 2) showed differential

behavior between the two studied species. For B, sorption and/or immobilization occurred slowly and steadily during the first 720 min, after which the relative speed increased until 1200 min when equilibrium and/or saturation was reached, remaining constant with a 90% removal. For Na, repetitive cycles of sorption/desorption with variable temporal durations were observed, but with a decreasing trend. Additionally, it was possible to identify the desorption of larger amounts of Na than those initially contained in the water (240 min), possibly due to the release of the inherent Na from the structural and compositional zeolite. The maximum removal percentage of Na did not exceed 35% in any of the experiments.

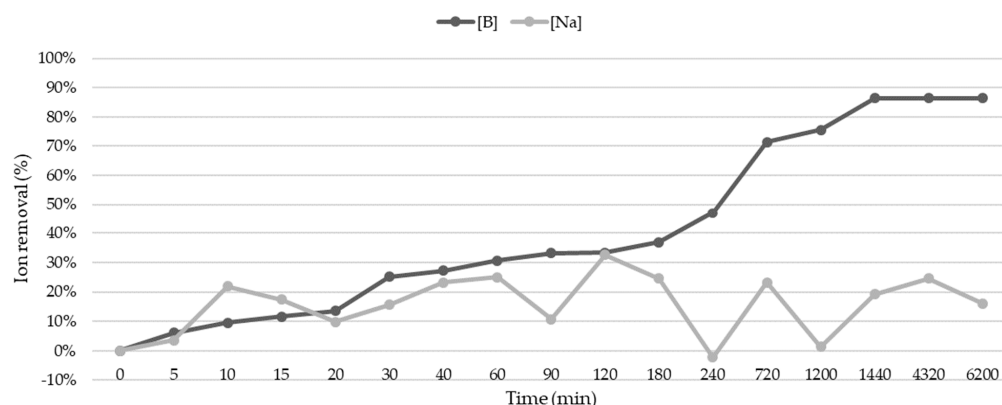


Figure 2. Removal of sodium and boron cations (%) on zeolite as a function of contact time.

3.4.2. Zeolite Effect on pH and Cation Removal

One of the factors that significantly influences sorption processes is undoubtedly the pH at which the process occurs, as it directly interferes with the behavior of charges susceptible to sorbent–sorbate interactions. The results showed a significant variation in the pH of irrigation water during the first 5 min of contact with zeolite, changing from an initial pH of 8.3 to 8 (Figure 3). After this time, the pH remained relatively constant at around 8 for the first 720 min, decreasing to 7.9 and remaining stable until the end of the test (6200 min). This slight decrease in the pH of irrigation water may help explain the low adsorption of sodium by zeolite. Rostamian et al. [64] identified that the sorption of sodium ions increases as the solution pH increases, due to the deprotonation process of various functional groups on the adsorbent. This results in more negatively charged sites, leading to greater electrostatic attraction between these sites and sodium, facilitating the sorption of the cation on the adsorbent’s surface. This trend is similar to that of boron, but with some nuances. Keren and Comunal [65] defined the maximum adsorption of boron at alkaline pH (9.3) but determined acceptable sorption in the pH range between 5.8 and 9.3. This would explain boron sorption by zeolite in irrigation water even with a pH < 9.3.

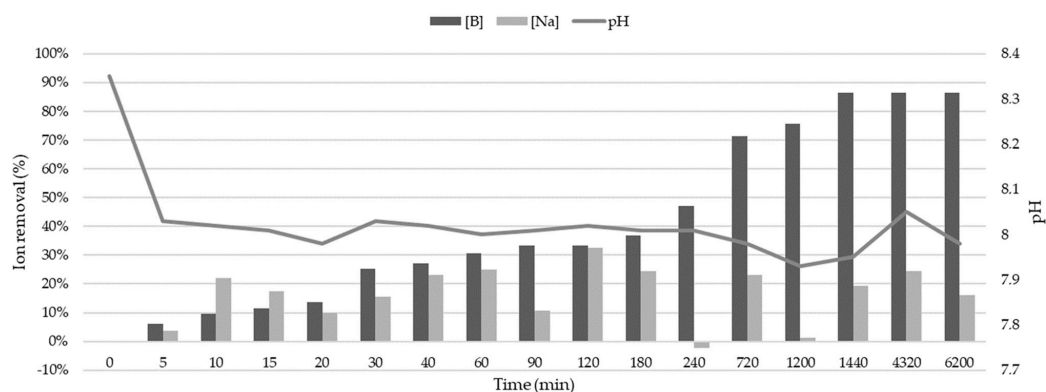


Figure 3. Water samples’ pH variation as a function of contact time with zeolite and its correlation with the percentages of boron (B) and sodium (Na) cation removal.

3.4.3. Kinetic Models

As mentioned earlier, kinetic data provide valuable information about sorbent/sorbate interactions and the mechanism governing or dominating the specific sorption process. In this study, the definition of sodium and boron removal kinetics by commercial zeolite was achieved by fitting the experimental results to the three most important kinetic models: pseudo-first-order, pseudo-second-order, and intraparticle diffusion. All models were evaluated based on their regression parameters R^2 to identify their applicability to the studied process. The results are presented in Table 8.

Table 8. Kinetic parameters for B and Na removal onto zeolite.

	Boron	Sodium
Pseudo-first-order		
R^2	0.9660	0.9406
K_1 (L min ⁻¹)	0.01	-0.20
q_e cal (mg g ⁻¹)	0.42	0.88
Pseudo-second-order		
R^2	0.9349	0.5913
K_2 (g mg ⁻¹ min ⁻¹)	-0.65	-0.03
q_e cal (mg g ⁻¹)	0.02	-0.34
h (mg g ⁻¹ min ⁻¹)	-1.86×10^{-4}	-3.78×10^{-3}
Intraparticle diffusion		
R^2	0.7902	0.3337
K_{in} (g mg ⁻¹ min ^{-1/2})	2.89×10^{-6}	0.028

where q_e represents the amount of sorbate retained (mg) per gram of sorbent at equilibrium; K_1 and K_2 are the rate constant of the pseudo-first-order and pseudo-second-order, respectively; and K_{in} is the rate of intraparticle diffusion.

For both ions, the correlation coefficients were below 0.79 for the intraparticle diffusion models, and in the case of sodium, also for the pseudo-second-order model. This indicated low representativeness and limited applicability for interpreting the experimental data. In other words, in these cases, the models were not suitable for describing the sorption kinetics. However, for both ions, the pseudo-first-order model showed correlation coefficients above 0.94, suggesting sorption kinetics of active site occupation governed by the surface reaction rate—essentially a physical or physisorption process [30,66]. Additionally, for boron, the pseudo-second-order model also exhibited an R^2 close to unity (0.9349), indicating the influence of chemical sorption or chemisorption as the rate-limiting step in the process's speed [61]. In this case, and accordance with the results obtained by Moussout et al. [67], it could indicate that the pseudo-first-order model is valid only in the initial adsorption stage and then transitions to chemisorption. The results obtained for the sorption of both cations on zeolite align with those reported in the literature for different types of zeolites, both natural and synthetic [29,31,32,67–69].

4. Conclusions

This study addressed the issue of water quality in an irrigation reservoir with high levels of boron (B) and sodium (Na)—9.7 and 0.75 meq/L, respectively—which adversely affect the development of sensitive crops such as citrus. It is crucial to highlight that this study, utilizing zeolite as a sorbent, was conducted in a context where this material was already employed as an agricultural soil amendment in southeastern Spain, an area where irrigation water quality is often compromised.

The results indicated that sodium removal exhibited limited efficiency (10–24%), with desorption observed in some cases, underscoring the challenges of combined removal

with boron and various elements present in natural irrigation waters. On the other hand, boron removal demonstrated higher efficiency (up to 100%) under specific conditions, with significant interactions and influences from other chemical species present in water and zeolite composition. Statistical analysis, including analysis of variance (ANOVA), identified significant factors for boron removal (zeolite content and contact time) but not for sodium. Based on statistical significance and practicality, optimal conditions for boron removal were determined as 4.93 g of zeolite/L and 723 min of contact time.

Kinetic studies revealed differential behaviors for sodium and boron, with cyclic sorption/desorption observed for sodium and slow, steady sorption for boron. The pseudo-first-order model was found to be applicable for both cations, indicating a physical or physisorption process, while the pseudo-second-order model suggested possible chemisorption for boron. pH variations during the process indicated a slight decrease, potentially explaining lower sodium adsorption, aligning with literature suggesting higher sodium adsorption at a higher pH.

The study paves the way for future research, particularly in understanding the complex interactions influencing the sorption behavior of sodium and boron on zeolite under dynamic conditions. The findings contribute to the optimization of zeolite-based treatments for agricultural irrigation water, providing insights into challenges and potential solutions for sodium and boron removal.

Author Contributions: Conceptualization, D.N.-G. and P.M.; data curation, D.N.-G.; formal analysis, D.N.-G.; funding acquisition, P.M.; investigation, D.N.-G. and P.M.; methodology, D.N.-G.; project administration, P.M.; software, D.N.-G.; supervision, J.J.M.-N. and P.M.; validation, P.L., V.L., A.C. and J.J.M.-N.; visualization, P.L.; writing—original draft, D.N.-G.; writing—review and editing, D.N.-G., J.J.M.-N. and P.M. All authors have read and agreed to the published version of the manuscript.

Funding: This study forms part of the AGROALNEXT program (AGROALNEXT2022/013, SIRIS Project) and was supported by MCIN with funding from European Union NextGenerationEU (PRTR-C17.I1) and by Generalitat Valenciana.

Institutional Review Board Statement: Not applicable.

Informed Consent Statement: Not applicable.

Data Availability Statement: The data presented in this study are available in the present work.

Conflicts of Interest: The authors declare no conflicts of interest.

References

1. Cataldo, E.; Salvi, L.; Paoli, F.; Fucile, M.; Masciandaro, G.; Manzi, D.; Masini, C.M.; Mattii, G.B. Application of Zeolites in Agriculture and Other Potential Uses: A Review. *Agronomy* **2021**, *11*, 1547. [[CrossRef](#)]
2. Nakhli, S.A.A.; Delkash, M.; Bakhshayesh, B.E.; Kazemian, H. Application of Zeolites for Sustainable Agriculture: A Review on Water and Nutrient Retention. *Water Air. Soil. Pollut.* **2017**, *228*, 464. [[CrossRef](#)]
3. Ramesh, K.; Reddy, D.D. Chapter Four—Zeolites and Their Potential Uses in Agriculture. In *Advances in Agronomy*; Sparks, D.L., Ed.; Advances in Agronomy; Academic Press: Cambridge, MA, USA, 2011; Volume 113, pp. 219–241.
4. Eroglu, N.; Emekci, M.; Athanassiou, C.G. Applications of Natural Zeolites on Agriculture and Food Production. *J. Sci. Food Agric.* **2017**, *97*, 3487–3499. [[CrossRef](#)] [[PubMed](#)]
5. Abadzic, S.D.; Ryan, J.N. Particle Release and Permeability Reduction in a Natural Zeolite (Clinoptilolite) and Sand Porous Medium. *Environ. Sci. Technol.* **2001**, *35*, 4502–4508. [[CrossRef](#)] [[PubMed](#)]
6. de Campos Bernardi, A.C.; Anção Oliveira, P.P.; de Melo Monte, M.B.; Souza-Barros, F. Brazilian Sedimentary Zeolite Use in Agriculture. *Microporous Mesoporous Mater.* **2013**, *167*, 16–21. [[CrossRef](#)]
7. Méndez-Argüello, B.; Lira-Saldivar, R.H.; Méndez-Argüello, B.; Lira-Saldivar, R.H. Uso potencial de la zeolita en la agricultura sustentable de la nueva revolución verde. *Ecosistemas Y Recur. Agropecu.* **2019**, *6*, 191–193. [[CrossRef](#)]
8. Akash, T.; Samvrudhi, K.; Upendra, R.; Riyaz, M. Biosensors for the Detection of Toxic Contaminants from Water Reservoirs Essential for Potable and Agriculture Needs: A Review. In Proceedings of the 2021 IEEE International Conference on Distributed Computing, VLSI, Electrical Circuits and Robotics (DISCOVER), NITTE, India, 19–20 November 2021; IEEE: NITTE, India, 2021; pp. 193–198.

9. Zaman, M.; Shahid, S.A.; Heng, L. Irrigation Water Quality. In *Guideline for Salinity Assessment, Mitigation and Adaptation Using Nuclear and Related Techniques*; Zaman, M., Shahid, S.A., Heng, L., Eds.; Springer International Publishing: Cham, Switzerland, 2018; pp. 113–131, ISBN 978-3-319-96190-3.
10. Malakar, A.; Snow, D.D.; Ray, C. Irrigation Water Quality—A Contemporary Perspective. *Water* **2019**, *11*, 1482. [[CrossRef](#)]
11. FAO Water Quality for Agriculture. Available online: <https://www.fao.org/3/t0234e/T0234E00.htm> (accessed on 19 October 2023).
12. Rodríguez Coca, L.I.; García González, M.T.; Gil Unday, Z.; Jiménez Hernández, J.; Rodríguez Jáuregui, M.M.; Fernández Cancio, Y. Effects of Sodium Salinity on Rice (*Oryza sativa* L.) Cultivation: A Review. *Sustainability* **2023**, *15*, 1804. [[CrossRef](#)]
13. Shah, A.; Wu, X.; Ullah, A.; Fahad, S.; Muhammad, R.; Yan, L.; Jiang, C. Deficiency and Toxicity of Boron: Alterations in Growth, Oxidative Damage and Uptake by Citrange Orange Plants. *Ecotoxicol. Environ. Saf.* **2017**, *145*, 575–582. [[CrossRef](#)]
14. Gupta, U.C. Boron Nutrition Of Crops. In *Advances in Agronomy*; Brady, N.C., Ed.; Academic Press: Cambridge, MA, USA, 1980; Volume 31, pp. 273–307.
15. Shireen, F.; Nawaz, M.A.; Chen, C.; Zhang, Q.; Zheng, Z.; Sohail, H.; Sun, J.; Cao, H.; Huang, Y.; Bie, Z. Boron: Functions and Approaches to Enhance Its Availability in Plants for Sustainable Agriculture. *Int. J. Mol. Sci.* **2018**, *19*, 1856. [[CrossRef](#)]
16. Yang, G. Sorption and Reduction of Hexavalent Uranium by Natural and Modified Silicate Minerals: A Review. *Env. Chem. Lett.* **2023**, *21*, 2441–2470. [[CrossRef](#)]
17. Eberle, S.; Schmalz, V.; Börnick, H.; Stolte, S. Natural Zeolites for the Sorption of Ammonium: Breakthrough Curve Evaluation and Modeling. *Molecules* **2023**, *28*, 1614. [[CrossRef](#)] [[PubMed](#)]
18. Kolmykova, L.I.; Nikashina, V.A.; Korobova, E.M. Experimental Study of the Sorption Properties of Natural Zeolite-Containing Tripolite and Their Ability to Purify Aqueous Solutions Contaminated with Ni and Zn. *Env. Geochem Health* **2023**, *45*, 267–274. [[CrossRef](#)] [[PubMed](#)]
19. Reich, R.; Danisi, R.M.; Kluge, T.; Eiche, E.; Kolb, J. Structural and Compositional Variation of Zeolite 13X in Lithium Sorption Experiments Using Synthetic Solutions and Geothermal Brine. *Microporous Mesoporous Mater.* **2023**, *359*, 112623. [[CrossRef](#)]
20. Norby, P. In-Situ XRD as a Tool to Understanding Zeolite Crystallization. *Curr. Opin. Colloid Interface Sci.* **2006**, *11*, 118–125. [[CrossRef](#)]
21. Stevens, R.W., Jr.; Siriwardane, R.V.; Logan, J. In Situ Fourier Transform Infrared (FTIR) Investigation of CO₂ Adsorption onto Zeolite Materials. *Energy Fuels* **2008**, *22*, 3070–3079. [[CrossRef](#)]
22. Mozgawa, W. The Influence of Some Heavy Metals Cations on the FTIR Spectra of Zeolites. *J. Mol. Struct.* **2000**, *555*, 299–304. [[CrossRef](#)]
23. Zijun, Z.; Effeney, G.; Millar, G.J.; Stephen, M. Synthesis and Cation Exchange Capacity of Zeolite W from Ultra-Fine Natural Zeolite Waste. *Environ. Technol. Innov.* **2021**, *23*, 101595. [[CrossRef](#)]
24. Falkenmark, M. Water and Mankind: A Complex System of Mutual Interaction. *Ambio* **1977**, *6*, 3–9.
25. Benjamin, S.R.; Junior, E.J.M.R.; de Lima, F.; Arruda, G.J. Nanobiosensors for Environmental Risk Assessment. In *Bionanomaterials for Environmental and Agricultural Applications*; IOP Publishing Ltd.: Bristol, UK, 2021. [[CrossRef](#)]
26. Pintó-Marijuan, M.; Turon-Orra, M.; González-Betancort, A.; Muñoz, P.; Munné-Bosch, S. Improved Production and Quality of Peppers Irrigated with Regenerated Water by the Application of 24-Epibrassinolide. *Plant Sci.* **2023**, *334*, 111764. [[CrossRef](#)]
27. Pashley, N.E.; Bind, M.-A.C. Causal Inference for Multiple Treatments Using Fractional Factorial Designs. *Can. J. Stat.* **2023**, *51*, 444–468. [[CrossRef](#)]
28. Antony, J. *Design of Experiments for Engineers and Scientists*; Elsevier: Amsterdam, The Netherlands, 2023; ISBN 978-0-443-15174-3.
29. Lyu, J.; Zhang, N.; Liu, H.; Zeng, Z.; Zhang, J.; Bai, P.; Guo, X. Adsorptive Removal of Boron by Zeolitic Imidazolate Framework: Kinetics, Isotherms, Thermodynamics, Mechanism and Recycling. *Sep. Purif. Technol.* **2017**, *187*, 67–75. [[CrossRef](#)]
30. Kluczka, J.; Trojanowska, J.; Zołotajkin, M. Utilization of Fly Ash Zeolite for Boron Removal from Aqueous Solution. *Desalination Water Treat.* **2015**, *54*, 1839–1849. [[CrossRef](#)]
31. Demirçivi, P.; Nasün-Saygili, G. Removal of Boron from Waste Waters Using HDTMA-Modified Zeolites. *Desalination Water Treat.* **2010**, *23*, 110–117. [[CrossRef](#)]
32. Wen, J.; Dong, H.; Zeng, G. Application of Zeolite in Removing Salinity/Sodicity from Wastewater: A Review of Mechanisms, Challenges and Opportunities. *J. Clean. Prod.* **2018**, *197*, 1435–1446. [[CrossRef](#)]
33. Paul, B.; Dynes, J.J.; Chang, W. Modified Zeolite Adsorbents for the Remediation of Potash Brine-Impacted Groundwater: Built-in Dual Functions for Desalination and PH Neutralization. *Desalination* **2017**, *419*, 141–151. [[CrossRef](#)]
34. Gunst, R.F.; Mason, R.L. Fractional Factorial Design. *WIREs Comput. Stat.* **2009**, *1*, 234–244. [[CrossRef](#)]
35. Weremfo, A.; Abassah-Oppong, S.; Adulley, F.; Dabie, K.; Seidu-Larry, S. Response Surface Methodology as a Tool to Optimize the Extraction of Bioactive Compounds from Plant Sources. *J. Sci. Food Agric.* **2023**, *103*, 26–36. [[CrossRef](#)] [[PubMed](#)]
36. Porter, J.F.; McKay, G.; Choy, K.H. The Prediction of Sorption from a Binary Mixture of Acidic Dyes Using Single- and Mixed-Isotherm Variants of the Ideal Adsorbed Solute Theory. *Chem. Eng. Sci.* **1999**, *54*, 5863–5885. [[CrossRef](#)]
37. Liu, Y.; Shen, L. From Langmuir Kinetics to First- and Second-Order Rate Equations for Adsorption. *Langmuir* **2008**, *24*, 11625–11630. [[CrossRef](#)]
38. Ho, Y.S.; McKay, G. Pseudo-Second Order Model for Sorption Processes. *Process Biochem.* **1999**, *34*, 451–465. [[CrossRef](#)]
39. Weber, W.J.; Morris, J.C. Kinetics of Adsorption on Carbon from Solution. *J. Sanit. Eng. Div.* **1963**, *89*, 31–59. [[CrossRef](#)]

40. Huang, L.; Yang, J.; Zhao, Y.; Miyata, H.; Han, M.; Shuai, Q.; Yamauchi, Y. Monolithic Covalent Organic Frameworks with Hierarchical Architecture: Attractive Platform for Contaminant Remediation. *Chem. Mater.* **2023**, *35*, 2661–2682. [[CrossRef](#)]
41. Montañó, C.; Montañó, J. *Advances in the Adsorption Capacity, Rupture Time and Saturation Curve of Natural Zeolites*; IntechOpen Limited: London, UK, 2023; ISBN 978-1-83768-515-8. [[CrossRef](#)]
42. Abdelrahman, E.A.; Alharbi, A.; Subaihi, A.; Hameed, A.M.; Almutairi, M.A.; Algethami, F.K.; Youssef, H.M. Facile Fabrication of Novel Analcime/Sodium Aluminum Silicate Hydrate and Zeolite Y/Faujasite Mesoporous Nanocomposites for Efficient Removal of Cu(II) and Pb(II) Ions from Aqueous Media. *J. Mater. Res. Technol.* **2020**, *9*, 7900–7914. [[CrossRef](#)]
43. Paris, E.C.; Malafatti, J.O.D.; Musetti, H.C.; Manzoli, A.; Zenatti, A.; Escote, M.T. Faujasite Zeolite Decorated with Cobalt Ferrite Nanoparticles for Improving Removal and Reuse in Pb²⁺ Ions Adsorption. *Chin. J. Chem. Eng.* **2020**, *28*, 1884–1890. [[CrossRef](#)]
44. Farghali, M.A.; Abo-Aly, M.M.; Salaheldin, T.A. Modified Mesoporous Zeolite-A/Reduced Graphene Oxide Nanocomposite for Dual Removal of Methylene Blue and Pb²⁺ Ions from Wastewater. *Inorg. Chem. Commun.* **2021**, *126*, 108487. [[CrossRef](#)]
45. Mubarak, M.F.; Mohamed, A.M.G.; Keshawy, M.; elMoghny, T.A.; Shehata, N. Adsorption of Heavy Metals and Hardness Ions from Groundwater onto Modified Zeolite: Batch and Column Studies. *Alex. Eng. J.* **2022**, *61*, 4189–4207. [[CrossRef](#)]
46. Derouane, E.G.; Védrine, J.C.; Pinto, R.R.; Borges, P.M.; Costa, L.; Lemos, M.A.N.D.A.; Lemos, F.; Ribeiro, F.R. The Acidity of Zeolites: Concepts, Measurements and Relation to Catalysis: A Review on Experimental and Theoretical Methods for the Study of Zeolite Acidity. *Catal. Rev.* **2013**, *55*, 454–515. [[CrossRef](#)]
47. Elaiopoulos, K.; Perraki, T.; Grigoropoulou, E. Mineralogical Study and Porosimetry Measurements of Zeolites from Scaloma Area, Thrace, Greece. *Microporous Mesoporous Mater.* **2008**, *112*, 441–449. [[CrossRef](#)]
48. Morante-Carballo, F.; Montalván-Burbano, N.; Carrión-Mero, P.; Espinoza-Santos, N. Cation Exchange of Natural Zeolites: Worldwide Research. *Sustainability* **2021**, *13*, 7751. [[CrossRef](#)]
49. Abou El-Defan, T.; El-Raies, S.; El-Kholy, H.; Osman, A. A Summary of Water Suitability Criteria for Irrigation. *J. Soil Sci. Agric. Eng.* **2016**, *7*, 981–989. [[CrossRef](#)]
50. Liu, G.; Dong, X.; Liu, L.; Wu, L.; Peng, S.; Jiang, C. Metabolic Profiling Reveals Altered Pattern of Central Metabolism in Navel Orange Plants as a Result of Boron Deficiency. *Physiol. Plant.* **2015**, *153*, 513–524. [[CrossRef](#)] [[PubMed](#)]
51. Cakmak, I.; Brown, P.; Colmenero-Flores, J.M.; Husted, S.; Kutman, B.Y.; Nikolic, M.; Rengel, Z.; Schmidt, S.B.; Zhao, F.-J. Micronutrients. In *Marschner's Mineral Nutrition of Plants*, 4th ed.; Rengel, Z., Cakmak, I., White, P.J., Eds.; Academic Press: San Diego, CA, USA, 2023; pp. 283–385, ISBN 978-0-12-819773-8.
52. Machado, R.M.A.; Serralheiro, R.P. Soil Salinity: Effect on Vegetable Crop Growth. Management Practices to Prevent and Mitigate Soil Salinization. *Horticulturae* **2017**, *3*, 30. [[CrossRef](#)]
53. Maas, E.V.; Grattan, S.R. Crop Yields as Affected by Salinity. In *Agricultural Drainage*; John Wiley & Sons, Ltd.: Hoboken, NJ, USA, 1999; pp. 55–108, ISBN 978-0-89118-230-6.
54. Munns, R.; Tester, M. Mechanisms of Salinity Tolerance. *Annu. Rev. Plant Biol.* **2008**, *59*, 651–681. [[CrossRef](#)] [[PubMed](#)]
55. Ashraf, M.; Harris, P.J.C. Photosynthesis under Stressful Environments: An Overview. *Photosynthetica* **2013**, *51*, 163–190. [[CrossRef](#)]
56. Ahluwalia, O.; Singh, P.C.; Bhatia, R. A Review on Drought Stress in Plants: Implications, Mitigation and the Role of Plant Growth Promoting Rhizobacteria. *Resour. Environ. Sustain.* **2021**, *5*, 100032. [[CrossRef](#)]
57. Maas, E.V. Salinity and Citriculture. *Tree Physiol.* **1993**, *12*, 195–216. [[CrossRef](#)]
58. Wilcox, L.V. *Classification and Use of Irrigation Waters*; U.S. Department of Agriculture: Washington, DC, USA, 1955.
59. Quist-Jensen, C.A.; Macedonio, F.; Drioli, E. Membrane Technology for Water Production in Agriculture: Desalination and Wastewater Reuse. *Desalination* **2015**, *364*, 17–32. [[CrossRef](#)]
60. Tan, S.; Jean, J.; Pralong, V.; Moldovan, S.; Guo, H.; Mintova, S. Effect of Particle Size on the Sodium Ions Utilization Efficiency of Zeolite-Templated Carbon as the Anode in a Sodium Ion Battery. *Cryst. Growth Des.* **2023**, *23*, 4065–4073. [[CrossRef](#)]
61. Núñez-Gómez, D.; Lapolli, F.R.; Nagel-Hassemmer, M.E.; Lobo-Recio, M.Á. Optimization of Fe and Mn Removal from Coal Acid Mine Drainage (AMD) with Waste Biomaterials: Statistical Modeling and Kinetic Study. *Waste Biomass Valor* **2020**, *11*, 1143–1157. [[CrossRef](#)]
62. Box, G.; Hunter, W.; Hunter, J. *Statistics for Experimenters: An Introduction to Design, Data Analysis, and Model Building*; Wiley: New York, NY, USA, 1992; ISBN 0-471-09315-7.
63. Khuri, A.I.; Mukhopadhyay, S. Response Surface Methodology. *WIREs Comput. Stat.* **2010**, *2*, 128–149. [[CrossRef](#)]
64. Rostamian, R.; Heidarpour, M.; Farhad, S.; Afyuni, M. Preparation, characterization and sodium sorption capability of rice husk carbonaceous adsorbents. *Fresenius Environ. Bulletin.* **2015**, *24*, 1649–1658.
65. Keren, R.; Communar, G. Boron Sorption on Wastewater Dissolved Organic Matter: PH Effect. *Soil Sci. Soc. Am. J.* **2009**, *73*, 2021–2025. [[CrossRef](#)]
66. Rudzinski, W.; Plazinski, W. Kinetics of Solute Adsorption at Solid/Solution Interfaces: A Theoretical Development of the Empirical Pseudo-First and Pseudo-Second Order Kinetic Rate Equations, Based on Applying the Statistical Rate Theory of Interfacial Transport. *J. Phys. Chem. B* **2006**, *110*, 16514–16525. [[CrossRef](#)] [[PubMed](#)]
67. Moussout, H.; Ahlafi, H.; Aazza, M.; Maghat, H. Critical of Linear and Nonlinear Equations of Pseudo-First Order and Pseudo-Second Order Kinetic Models. *Karbala Int. J. Mod. Sci.* **2018**, *4*, 244–254. [[CrossRef](#)]

68. Yüksel, S.; Yürüm, Y. Removal of Boron from Aqueous Solutions by Adsorption Using Fly Ash, Zeolite, and Demineralized Lignite. *Sep. Sci. Technol.* **2009**, *45*, 105–115. [[CrossRef](#)]
69. Siemens, A.M.; Dynes, J.J.; Chang, W. Sodium Adsorption by Reusable Zeolite Adsorbents: Integrated Adsorption Cycles for Salinised Groundwater Treatment. *Environ. Technol.* **2021**, *42*, 3083–3094. [[CrossRef](#)]

Disclaimer/Publisher’s Note: The statements, opinions and data contained in all publications are solely those of the individual author(s) and contributor(s) and not of MDPI and/or the editor(s). MDPI and/or the editor(s) disclaim responsibility for any injury to people or property resulting from any ideas, methods, instructions or products referred to in the content.